AGU PUBLICATIONS

JGR

Journal of Geophysical Research: Atmospheres

RESEARCH ARTICLE
10.1002/2016JD025562

Key Points:
- Climatology of full spectrum of tropical cyclone track directions analyzed for the Australian region
- The MJO influences the climatology of westward and eastward moving TCs
- Potential for subseasonal forecast applications given the month and MJO phase

Correspondence to:
S. L. Lavender,
Sally.Lavender@csiro.au

Citation:
Lavender, S. L., and A. J. Dowdy (2016), Tropical cyclone track direction climatology and its intraseasonal variability in the Australian region, *J. Geophys. Res. Atmos.*, *121*, 13,236–13,249, doi:10.1002/2016JD025562.

Received 23 JUN 2016
Accepted 28 OCT 2016
Accepted article online 2 NOV 2016
Published online 18 NOV 2016

Tropical cyclone track direction climatology and its intraseasonal variability in the Australian region

Sally L. Lavender[1] and Andrew J. Dowdy[2]

[1]CSIRO Climate Science Centre, Aspendale, Victoria, Australia, [2]Bureau of Meteorology, Melbourne, Victoria, Australia

Abstract Aspects of tropical cyclone (TC) activity, such as the influence of the El Niño-Southern Oscillation and the variability of TC genesis location, have been examined in numerous previous studies. However, relatively few studies have examined aspects such as the influence of intraseasonal variability on TC track direction. Here we focus on a number of knowledge gaps relating to observed TC track directionality and intraseasonal variability in the Australian region. Climatological examinations are presented for TC track directional variability throughout the Australian region. In contrast to previous studies that have focused on the mean direction of TC movement in this region, TC tracks are examined here based on the full spectrum of track directions for a given location or region. Variability in initial TC track directions is investigated, including an examination of the influence of the Madden-Julian oscillation (MJO). It is demonstrated that there is a considerable degree of seasonal and intraseasonal variation in TC motion in this region. These variations result from variations in genesis location throughout the TC season, as well as zonal wind anomalies associated with the influence of the MJO on the steering flow winds. Anomalous westerly steering flow occurs during MJO phase 4 – 5 and anomalous easterly flow during phase 8 – 1 in the western basin, with resulting changes in the proportion of TC tracks in each direction during these phases of the MJO. The results presented here are intended to provide improved seasonal TC activity guidance and enhanced resilience to TC impacts.

1. Introduction

Tropical cyclones (TCs) and the associated extreme weather (including extreme winds, storm surge, and heavy rainfall) can have devastating impacts on various regions throughout the world. There are also beneficial effects, such as water availability, given they can provide a significant proportion of the total mean rainfall in some locations [*Lavender and Abbs*, 2013]. An ability to manage the regional TC impacts depends on an understanding of the factors that drive TC variability. This variability can occur over a wide range of temporal scales, including those pertaining to daily, seasonal, annual, and multidecadal processes. Some aspects of TC activity are at present poorly understood, particularly in relation to intraseasonal variability; thus, there is considerable scope for improvements in knowledge that could potentially lead to improved TC preparedness.

The Australian area of responsibility for TC analysis and forecasting, as recognized by the World Meteorological Organization (WMO), comprises the longitude range from 90°E to 160°E in the Southern Hemisphere (SH). Between 1970 and 2013, TCs have resulted in insurance losses of $5.3 billion for the Australian continent [*Productivity Commission*, 2014]. TCs in the Australian region show a number of unique characteristics, including relatively large variability in their direction and speed as compared to other regions of the world [*Bessafi et al*., 2002], notable difficulties in predicting TC tracks in this region [*Pike and Neumann*, 1987], and a majority of systems forming relatively close to land resulting in a large proportion of TCs making landfall [*McBride and Keenan*, 1982]. Additionally, the southwest Pacific region, encompassing the eastern part of the Australian region, exhibits a considerably high proportion of eastward moving TCs [*Holland*, 1984b]. *Dare and Davidson* [2004] produced a detailed analysis of 40 years of TC tracks in the Australian region, updating previous literature on characteristics of TCs in the region [e.g., *Holland*, 1984b; *McBride and Keenan*, 1982].

The majority of studies analyze TC numbers and genesis, with fewer studies examining track behaviors. *Holland* [1984b] analyzed the direction and speed of tropical storms, hurricanes, and major hurricanes in the Australian and South Pacific regions over the early TC record between 1958 and 1979. Additionally, dynamical and thermal structures of these systems, separated by intensity, were analyzed. *Ramsay et al*. [2012] examined Southern Hemisphere tracks using a cluster analysis technique. Four (out of seven) clusters

included tracks from the Australian region, but the clusters were heavily influenced by initial location rather than the actual track characteristics. They analyzed the large-scale environmental variables influencing genesis in each cluster and found links with both the El Niño–Southern Oscillation (ENSO) and the Madden-Julian oscillation (MJO), confirming previous studies in the region. The same cluster technique was also applied over the Fiji region (east of our area of interest), finding modulation of tracks by ENSO [*Chand and Walsh*, 2009] and the MJO [*Chand and Walsh*, 2010].

Previous studies that have also considered regional variations in TC track direction typically divide a region up into evenly spaced boxes and calculate the average track direction per box [e.g., *Hall et al*., 2001; *Dowdy et al*., 2012]. Although mean values can be useful for some applications, it is noted that a considerable amount of information is lost during this averaging process which could be valuable to retain in some cases, particularly in locations such as the Australian region where there exists a relatively large variability in the tracks [*Dare and Davidson*, 2004]. Consequently, TC tracks are examined here based on the full spectrum of track direction for a given location or region, with a view toward this information being of relevance to applications such as probabilistic risk assessments in relation to TC track variability on a range of different temporal scales.

Numerical weather prediction (NWP) models are used by the Australian Bureau of Meteorology (BoM) to forecast TC genesis and predict their tracks throughout the Australian region at relatively short lead times, ranging from minutes (i.e., nowcasting) up to several days. On seasonal time scales, forecasts are also produced operationally by BoM with some predictive skill being derived from the influence on TC activity of large-scale atmospheric and oceanic modes of variability, such as ENSO and the Indian Ocean Dipole (IOD) [e.g., *Nicholls*, 1979, 1984; *Evans and Allan*, 1992; *Basher and Zheng*, 1995; *Kuleshov et al*., 2008; *Ramsay et al*., 2008; *Dowdy*, 2014; *Liu and Chan*, 2012; *Werner et al*., 2012].

There have been considerable recent efforts toward seamless forecasting ability across a wide range of time scales [e.g., *Vitart*, 2014; *Robertson et al*., 2015; *Zhu et al*., 2014], further highlighting the importance of understanding the variability of TC activity across a range of temporal scales. Intraseasonal time scales of the order of a week to a few months span the gap between weather forecasting time scales and those of seasonal prediction. The MJO is known to modulate TC numbers globally on intraseasonal time scales, with increased TC activity when the active phase is over the study region [*Frank and Roundy*, 2006; *Zhang*, 2013]. This link between the MJO and TC numbers has been confirmed for the Australian region [e.g., *Hall et al*., 2001; *Leroy and Wheeler*, 2008; *Camargo et al*., 2009; *Vitart et al*., 2010; *Diamond and Renwick*, 2014]. The increase in activity is linked to various changes in the background environmental conditions, such as enhanced cyclonic anomalies in the 850 hPa relative vorticity associated with the equatorial Rossby wave response to the MJO convective heating anomalies [*Hall et al*., 2001]. However, there are considerable knowledge gaps on TC activity relating to this temporal scale (e.g., as noted by *Bessafi and Wheeler* [2006]), indicating a clear need for investigations of the intraseasonal variability of both TC activity and motion.

Although many previous studies have examined relationships between the MJO and TC numbers and genesis in various regions of the world, relatively few have focussed on TC track. The studies that have examined MJO and track direction have predominantly been for the western North Pacific region [*Chen et al*., 2009; *Kim et al*., 2008; *Li and Zhou*, 2013; *Wu et al*., 2013; *Yang et al*., 2015]. The few studies that have examined the relationships between the MJO and TC track direction in Southern Hemisphere regions [*Hall et al*., 2001; *Ho et al*., 2006; *Chand and Walsh*, 2010] have not presented climatologies based on individual TC track directions, with their analyses primarily focussed on variations in TC genesis and track density rather than track direction.

This study focuses on TC tracks and their directional variability. Climatological examinations are presented of TC track directions throughout the Australian region. In contrast to previous studies that have focussed on the mean direction of TC movement in this region, a novel feature of the analyses presented here is that the full spectrum of TC track directions is considered. In particular, the intraseasonal variability of TC activity in this region is examined, with a focus on initial TC track direction. The drivers of this variability are investigated, including factors such as variations in genesis regions, as well as the influence of the MJO. The results are intended to provide guidance on predicting TC activity in this region, spanning the Southeast Indian and Southwest Pacific regions.

The following section describes the data and methods used. Section 3 examines the climatology of TC track direction and translational speed. Intraseasonal variations in the proportion of eastward and westward

moving tracks are analyzed, and the relationships between the MJO and these variations are examined. Section 4 discusses these results and provides some concluding remarks including possible future work.

2. Data and Methods

2.1. TC Best Track Data

TC data for the Australian region, from 90°E to 160°E, come from the International Best Track Archive for Climate Stewardship v03r06 (IBTrACS) [*Knapp et al*., 2010]. The TC season in the SH is from July to June, labeled by the year it ends. The Australian TC season is typically considered to span months from November to April (with peak activity in January to March), while noting that TCs which occur outside of this period are also considered as occurring within that particular TC season. TC data are examined here for 43 tropical cyclone seasons: from the 1971 TC season until the 2013 TC season (i.e., from 1 July 1970 to 30 June 2013). This time period only includes the satellite era, with TC tracks being more reliable during this period than during earlier time periods for this region [e.g., *Dowdy and Kuleshov*, 2012]. During this time there will still be inhomogeneities in the data due to improvements in satellite observations and changes in the analysis techniques such as implementation of the Dvorak technique. *Harper et al*. [2008] give an overview of significant events influencing the accuracy of TC location and intensity estimates. As in previous studies examining TC activity in the SH [e.g., *Dowdy et al*., 2012; *Ramsay et al*., 2012], analysis involving intensity only considers data from the 1982 TC season onward due to a considerably lower reliability of this information for earlier time periods.

In cases where the temporal frequency of detections in the database differs from the 6-hourly regular time steps contained for the majority of systems (i.e., 00 UTC, 06 UTC, 12 UTC, and 18 UTC), the location and intensity information were interpolated to match this regular 6-hourly time. Landfall is considered as the first location of the track that intersects with land, i.e., where the eye crosses the land (to the nearest 6 h).

The primary focus of this study is on the track directions, rather than the genesis. Some of the analysis presented here includes examinations of track directions based on their net zonal movement being either "eastward" or "westward" during the initial 48 h period of their recorded track. For consistency throughout the data set, we consider the origin of a TC track (i.e., its genesis) as the first point of the track recorded in the IBTrACS database over ocean, noting that a relatively small amount of tracks are first recorded over land regions. This will, in most cases, be prior to reaching the Australian classification of TC intensity (17.5 m s^{-1} [34 kt]) with average wind speeds and minimum pressures for this initial point (as calculated from the 1982 season onward) of 14.7 m s^{-1} [29 kt] and 1000 hPa, respectively. This definition allows us to use the data from the 1970s when the intensity data are less reliable than the more recent time periods. The analysis was also performed, and results discussed, using TC genesis defined by intensity (wind speeds greater than 17.5 m s^{-1} or minimum pressure below 996 hPa if wind speed information is unavailable) from the 1982 TC season onward.

2.2. Atmospheric Data

Background environmental (steering) flow was calculated using zonal and meridional winds from the ERA-Interim reanalysis obtained from the European Centre for Medium-Range Weather Forecasts (ECMWF) on a 0.75° × 0.75° grid [*Dee et al*., 2011]. Following the method of a number of previous studies [*Holland*, 1984a; *Carr and Elsberry*, 1990; *Zhao et al*., 2009], the steering flow is calculated at 6-hourly intervals throughout the study period for all grid locations in the region based on the pressure-weighted wind fields from 850 hPa to 300 hPa (i.e., horizontal wind fields at 850 hPa, 700 hPa, 500 hPa, and 300 hPa).

2.3. The MJO

The real-time multivariate MJO index of *Wheeler and Hendon* [2004] is used here to examine the influence of the MJO on TC tracks. The index comprises eight different phases, representing the eastward near-equatorial propagation of the MJO as measured in anomalies of tropospheric zonal winds and outgoing long-wave radiation (OLR). This index is available from the 1975 TC season onward (representing the period of available OLR data from satellite observations used for defining the MJO phases). The MJO phases are grouped as in previous studies [*Leroy and Wheeler*, 2008; *Camargo et al*., 2009; *Ramsay et al*., 2012], with adjacent phases being combined to make four categories (phases 8 + 1, 2 + 3, 4 + 5, and 6 + 7), which increases the sample size for each category. In addition, a "weak MJO" category is defined when the amplitude of the *Wheeler and*

Table 1. Influence of MJO Phase on Northern Australia, Based on Data From *Wheeler et al.* [2009] and *Hall et al.* [2001]

MJO Phase Influence on Northern Australia	Phase 8 – 1	Phase 2 – 3	Phase 4 – 5	Phase 6 – 7
OLR anomalies	Positive	Positive (east)	Negative	Negative (east)
Rainfall	Decreased	Decreased	Increased	Increased in east
Winds	Little change	Easterly anomalies	Westerly anomalies	Westerly anomalies
TC activity	Decreased	Small decrease	Increased in west	Increased in east

Hendon [2004] index is less than 1. The influence of the phase of the MJO on weather over northern Australia, including precipitation and TCs, is shown in Table 1.

3. Results

3.1. TC Track Climatology

A climatology of 6-hourly TC track direction and translational speed is presented in this section. This incorporates 464 TCs (14660 six-hourly events) that originated in the Australian region during the 43 year study period comprising the TC seasons from 1971 to 2013. The TC tracks are shown in Figure 1a. The Australian region is further categorized into three smaller regions (black lines Figure 1a), similar to those used by BoM for operational forecasting purposes and as examined previously by *Dare and Davidson* [2004].

The number of TCs originating in each of the three regions (black names and numbers) is shown in Figure 1a, indicating that the west is the most active region with 228 TCs during the study period, as compared to 122 in the central region and 114 in the eastern region. The number of these TCs that make landfall on the Australian continent is also shown, with 94 TCs making landfall in the central region (i.e., 77% of the total number for this region), noting that this relatively high number reflects the close proximity of genesis to land in this region. In contrast to the central region, only 61 (27%) TCs make landfall in the western region and 40 (35%) in the eastern regions. In total for the entire Australian region, 322 (69%) of the TCs come within 5° of the Australian continent, also noting that over a quarter of the TCs that make landfall ultimately make landfall multiple times.

Figure 1b shows the relative frequency of occurrence of TC tracks in a given direction, shown for eight individual direction ranges each of 45° in range (i.e., corresponding to the cardinal and intermediate directions: north, northeast, east, southeast, south, southwest, west, and northwest). These distributions are presented individually for regions of $10 \times 10°$ in latitude and longitude. The length of the bar for a particular direction represents the proportion of TCs moving in that direction, where direction is away from the center of the plot. The width of the "fans" highlights the number of detections in that grid box relative to the whole region with the red (blue) numbers showing the total number of TC detections and if storms are on average intensifying (dissipating). The colored shading indicates the translational speed distribution of the TC tracks in a given direction, with red representing the proportion of faster speeds and blue representing the proportion of slower speeds, as well as a range of intermediate color for the intermediate speeds (as shown in the key provided).

The track directions are predominantly westward between about 10°S and 20°S in the western region, while in the eastern region the distributions generally show a somewhat higher degree of variability in direction. There is an almost equal split in the direction of movement in some grid boxes, such as over the Gulf of Carpentaria (i.e., at 140°E, 10°S), noting that this provides an example of where the track information can be almost completely lost when considering the mean direction (as shown by the white arrows in Figure 1b).

Intensification of the systems typically occurs in the 10°S latitude band as shown by the red numbers in Figure 1b (based on a mean decrease in central pressure), with TCs tending to decay (blue numbers, Figure 1b) at latitudes farther to the south. Recurvature of tracks is evident from the shift in direction between 20°S and 30°S, with the red colors in the "fans" showing that the translational speed tends to increase after tracks make extratropical transition south of about 30°S.

Although tracks that form in the Gulf of Carpentaria are unique in some respects, including due to a large proportion making landfall, the distributions presented in Figure 1b indicate that the direction that these tracks take in the 10°S band (i.e., prior to landfall) is more similar to those to the east than west of 135°E. At 10°S, over 40% of TCs in the Gulf of Carpentaria move in an eastward direction to the east of 135°E and less than 15% in

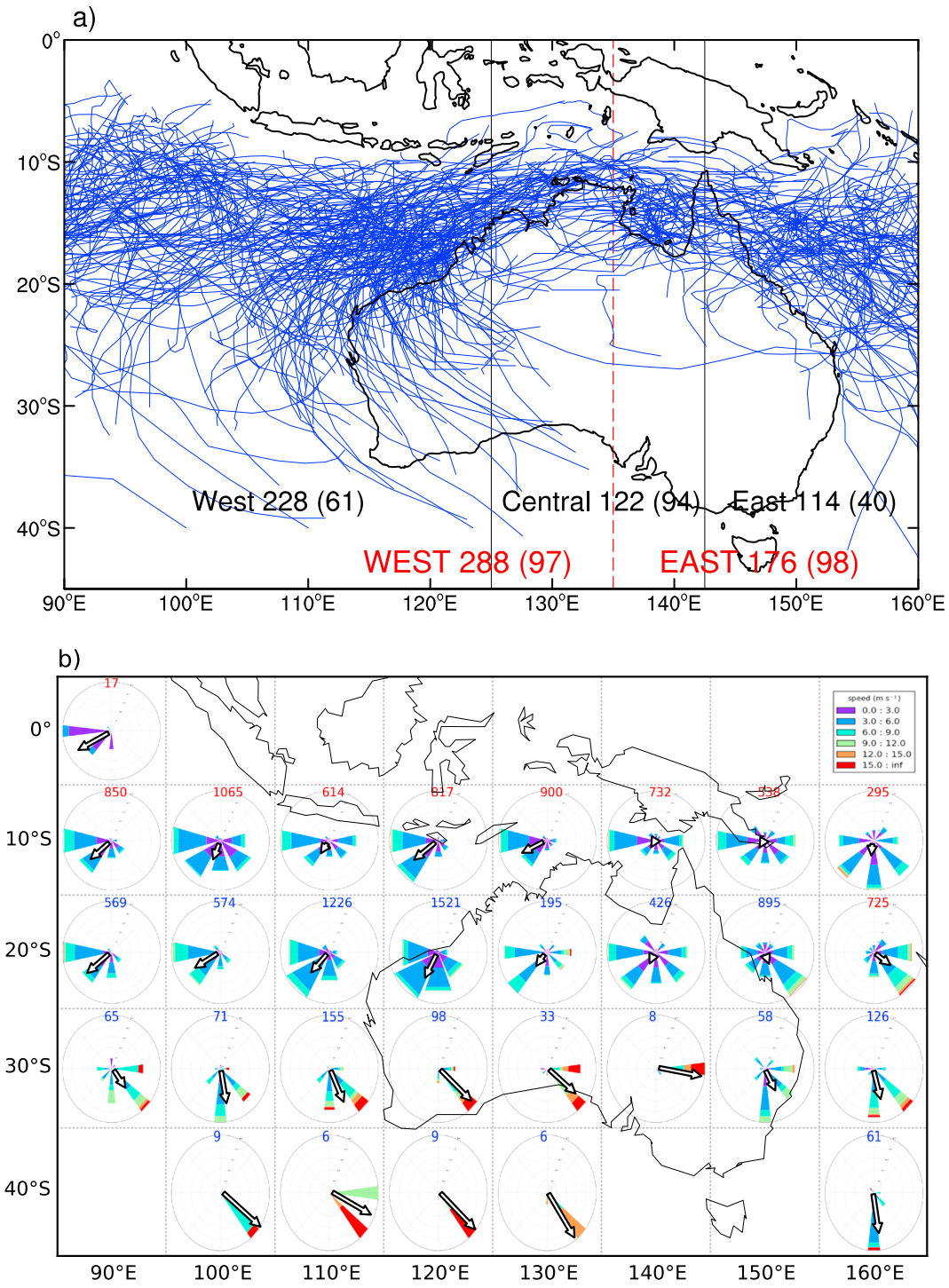

Figure 1. (a) Map showing all tracks that originate in the Australian region during the study period from the 1971 to 2013 TC season in the SH. Black lines and numbers indicate the numbers of TC numbers in the three smaller regions (western, central, and eastern regions) based on the location of origin for each TC track, with the number of these TCs that go on to make landfall on the Australian continent also shown (in brackets) for each region. Red lines and numbers show the same but for the two regions used in this study. (b) Polar plots for each 10 × 10° boxes for the Australian region, showing the relative proportion of translational TC tracks in eight different directions (length of fans). These directional distributions are based on 6-hourly TC data. The distribution of TC translation speed is also shown for each direction (from slow (blue) to fast (red) as shown in the legend). The numbers listed for each 10 × 10° box represent the number of 6 h TC occurrences at each location during the study period, with the color of the numbers showing regions where TCs are intensifying (red) or dissipating (blue) on average. The width of the fan also indicates the relative number of TCs in that grid box compared to the entire region. The black and white arrows represent the mean vector direction and magnitude of the TC movement.

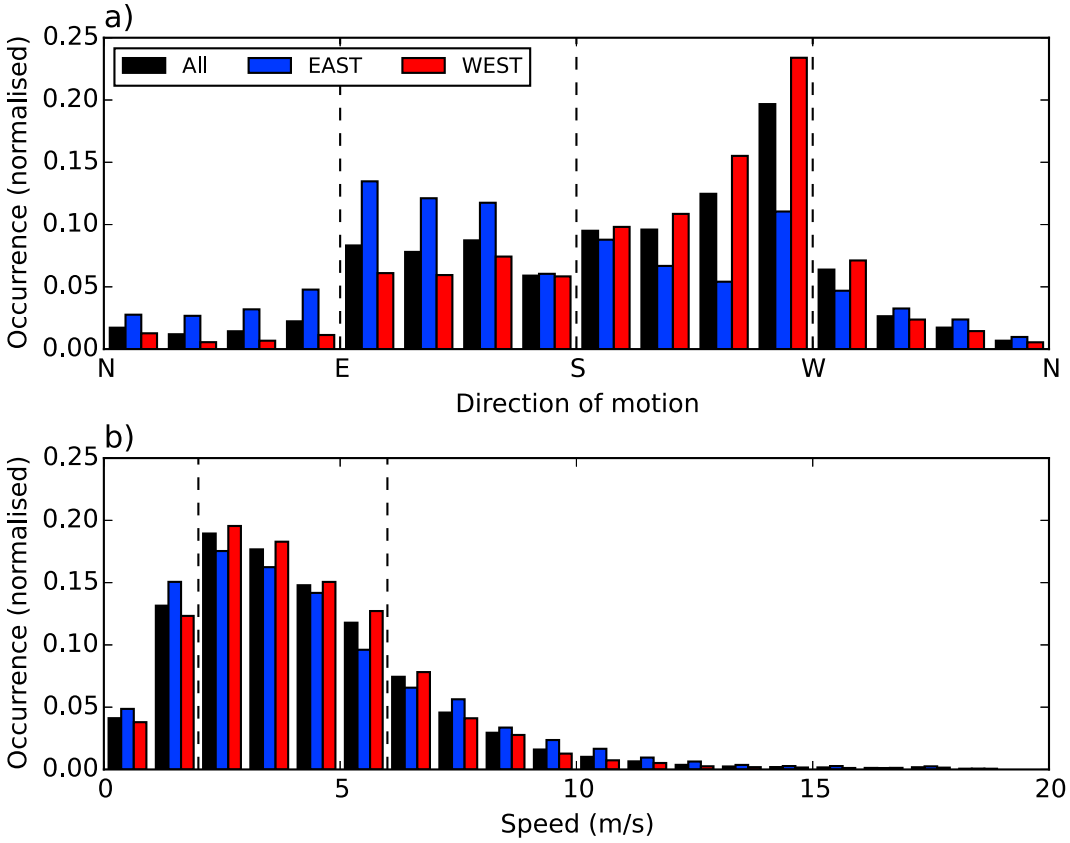

Figure 2. Distribution of (a) direction and (b) speed for all (black), EAST (blue), and WEST (red) basin TCs (1970–2012). Normalized such that the sum of all bins for each basin equals unity. Dashed lines in Figure 2b at 2 m s^{-1} and 6 m s^{-1} referred to in the text.

the grid boxes to the west of 135°E. Consequently, for the analyses presented in subsequent parts of this paper, the Australian region has been categorized into two basins either side of 135°E in longitude: i.e., a western basin (WEST; from 90°E to 135°E) and an eastern basin (EAST; from 135°E to 160°E). This boundary is included in Figure 1a (red, dashed line), with the numbers originating and making landfall in the two basins also included (red names and numbers). There are 288 and 176 TCs originating in the WEST and EAST regions, respectively, with 34% and 56% of these making landfall.

Figure 2 shows the distribution of translational direction and speed for all TCs (black) and split into WEST (red) and EAST (blue) basins. When considering the directional distribution for all tracks (Figure 2a), there is a peak in the west to southwest direction, with this being associated with the larger number of TCs in WEST (where the direction is predominantly west to southwest) than the EAST. In contrast, EAST shows a peak in east to southeast direction. This difference between WEST and EAST is consistent to some degree with what could be expected based on the presence of land, with the central location of the Australian continent acting to favor longer westward tracks in WEST and longer eastward tracks in EAST, due to dissipation of TC intensity over land. However, the actual reason may not be quite that simple. When this analysis is repeated using information only from the initial 48 h or initial 24 h of the track (i.e., to reduce the potential influence of very long tracks), the distribution (not shown) remains similar in shape to that in Figure 2.

The mean speed is approximately 4.3 m s^{-1} for the entire Australian region, with values of 4.2 m s^{-1} and 4.4 m s^{-1} in the WEST and EAST basins, respectively (Figure 2b). These speeds are consistent with results presented in previous studies [*Dare and Davidson*, 2004]. EAST has a larger spread in the range of speeds that occur, with relatively higher proportions of TCs at both tails of the speed distribution (i.e., very slow and very fast) as compared to WEST. WEST has a larger proportion of TCs moving at speeds between 2 m s^{-1} and 6 m s^{-1} (shown by dashed lines in Figure 2b), while EAST has a larger proportion of TCs moving at speeds outside of this range.

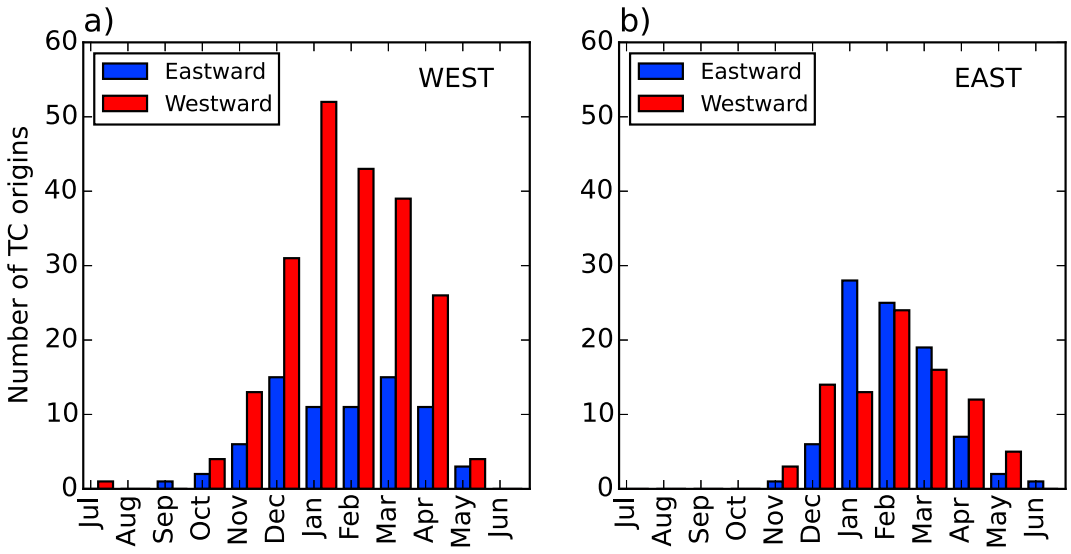

Figure 3. Number of eastward (blue) and westward (red) TC tracks, based on their net zonal moment during the first 48 h of the track. This is shown individually for each month in (a) WEST and (b) EAST basins.

3.2. Intraseasonal Variation in Westward and Eastward Tracks

For subsequent analyses the track data have been categorized as westward or eastward, based on their net direction of zonal motion over the initial 48 h period (as described in section 2.1). Figure 3 shows the number of westward and eastward tracks during the study period, presented individually for each month and for the WEST and EAST basins. In WEST, there are 213 westward and 75 eastward moving tracks, while in EAST there is a more similar proportion of westward and eastward moving TCs with 87 westward moving and 89 eastward moving.

The increase in TC activity in the summer is clearly evident, with largest numbers occurring during January to March. However, in WEST the number of eastward moving systems remains relatively constant between December and April, with increases in the number of westward moving tracks occurring between January and March. In EAST, the number of eastward moving tracks is highest in January and February, while the number of westward moving systems is highest in February and March. The ratio of eastward to westward moving systems is enhanced in EAST from January to March (Figure 3 and Table 2) relative to the months before and after, with the largest percentage of eastward tracks occurring during January (i.e., 68%).

With the advance of the monsoon in December toward Australia, the monsoon shear line (Figure 4) moves poleward bringing conditions that are more favorable for TC formation north of the shear line, as well as bringing westerly flow farther poleward, thereby enhancing the potential for eastward TC track directions. This corresponds well with percentage of eastward moving TCs in EAST (Table 2) but not with the location of formation of these TCs which are generally south of the shear line. In WEST there is a decrease in the percentage of eastward TCs, especially poleward of 12.5°S during January and February which also cannot be explained by the variations in the monsoon shear line and associated background steering flow. Alternatively, this is likely associated with the location of formation of TCs at this time of the year. For example, Figure 4 shows the initial location of the westward and eastward moving systems for the months from November to April and the average

Table 2. Summary of Figures 3 and 4[a]

	Nov		Dec		Jan		Feb		Mar		Apr	
% of All Storms	5		14		22		22		19		12	
% E moving WEST/EAST	32	25	33	30	17	68	20	51	28	54	30	37
% E moving 0–12.5°S WEST/EAST	32	25	33	13	26	33	33	73	29	45	29	40
% E moving 12.5–25°S WEST/EAST	n/a	n/a	30	42	9	73	10	45	26	58	33	25

[a]Percentage of storms falling in each month from November to April and corresponding percentage of eastward moving tracks for the two basins, WEST and EAST. Additionally the percentage of eastward moving systems split at 12.5°S is shown for WEST and EAST.

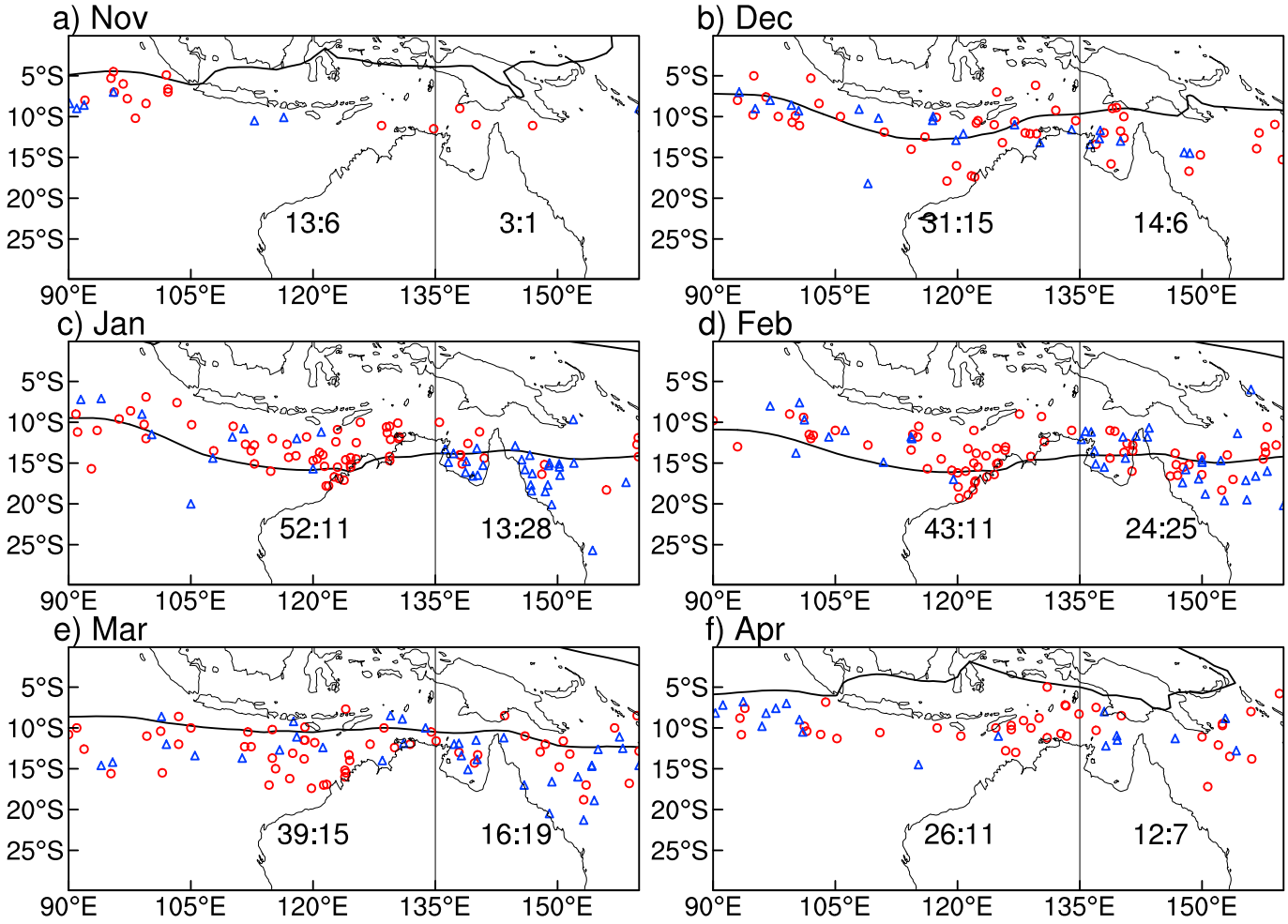

Figure 4. Locations of TC origins for eastward (blue triangle) and westward (red circle) moving systems during the study period. Also shown for each month is the number of westward and eastward moving TCs, listed separately for the western and eastern basins. The boundary line between WEST and EAST is shown at 135°E. The black line indicates the average location of the monsoon shear line calculated from the 850 hPa winds.

location of the 850 hPa monsoon shear line. A southward shift in the location of origin is evident in the central summer months due to the poleward shift in location of the monsoon shear line. This poleward shift in genesis results in TCs forming closer to land such that the appearance of more westward than eastward TCs in WEST could result from eastward moving systems making landfall before developing into a TC. This is also true for EAST with more eastward moving systems in the central summer months.

3.3. Influence of the MJO

The relationship between the MJO and the direction of movement of TCs in the Australian region is examined in this section. Figure 5, summarized in Table 3, presents the westward and eastward tracks occurring during the different phases of the MJO. Decreased activity in phase 8 – 1 and increased activity in phase 4 – 5 is clearly evident, consistent with previous studies (such as *Hall et al.* [2001] and *Camargo et al.* [2009]). It is also suggested from the results presented in Figure 5 and Table 3 that the ratio of eastward to westward moving TCs differs between the different MJO phases in some cases.

Considering the results for WEST, there are relatively few eastward moving systems for phase 8 – 1, with only three of the total of 20 systems (i.e., 15%) moving eastward. The proportion of eastward systems increases (to 21%) for phase 2 – 3 (anomalous easterlies, see Table 1), particularly toward the western boundary of WEST. For phase 4 – 5 (anomalous westerlies), locations with a relatively high proportion of eastward moving systems extend across much of the western basin (representing 38% of all systems) but are confined to

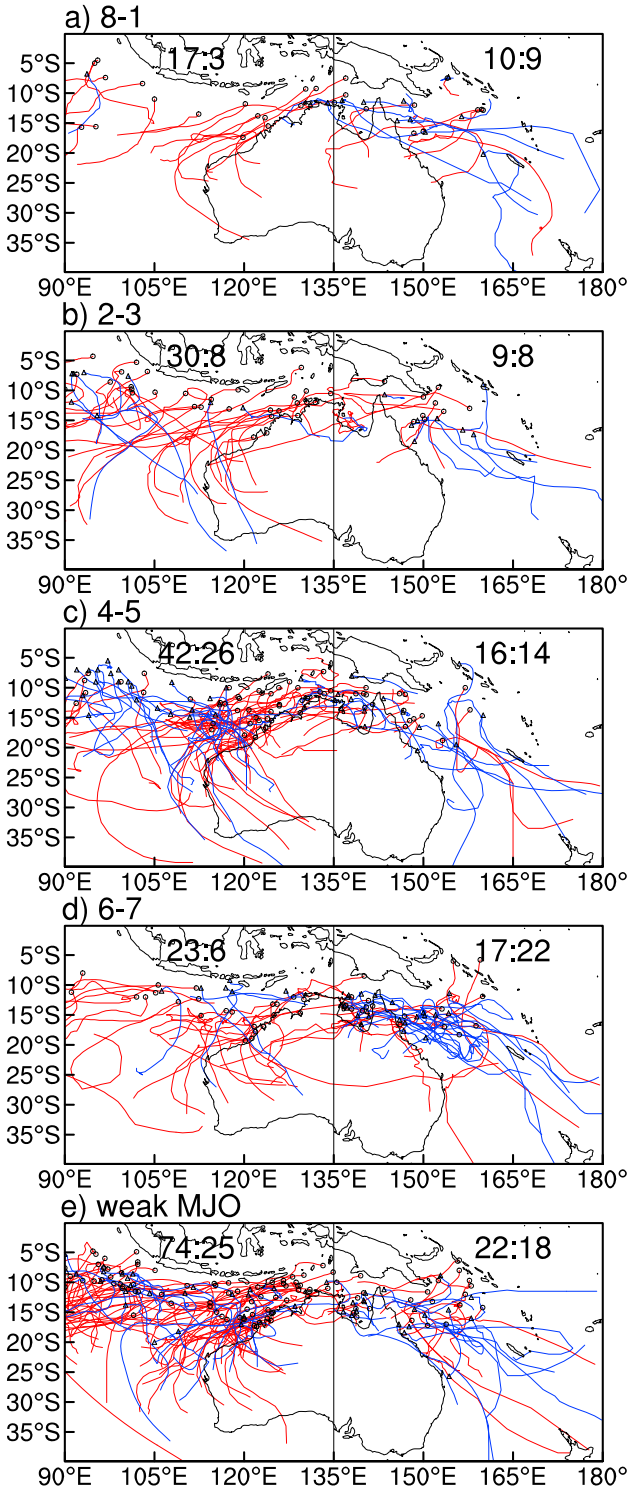

Figure 5. Westward (red) and eastward (blue) moving TCs during different MJO phases. Also shown are the numbers of westward and eastward moving TCs in each case, listed separately for the western and eastern basins. The boundary line between the WEST and EAST basins is shown at 135°E.

the eastern part of WEST for phase 6 – 7 (representing 20% of all systems in the western basin). In the weak MJO amplitude category (Figure 5e), locations with relatively high proportions of eastward moving systems extend across much of WEST, with a total of 25% of systems moving eastward for this MJO category in WEST. When split by latitude at 12.5°S (Table 3), this increase (decrease) in eastward TCs during phase 4 – 5 (8 – 1) is not notably different between the northern and southern regions, suggesting that the latitude of formation is not playing a large role in the MJO influence on direction of movement. When TC genesis is defined by intensity (see section 2.1), the influence of the MJO on the variation in track directions is even more pronounced, with westward to eastward track ratios of 12:1 and 26:15 for phase 8 – 1 and phase 4 – 5, respectively, with a clearer eastward propagation of the proportion of eastward moving TCs (while noting the smaller sample size).

In EAST, there is some indication of an influence of the MJO on track direction, although the variations are not as pronounced as the case for WEST. However, there is some suggestion in EAST of an increase in the proportion of eastward moving TCs during phase 6 – 7 (anomalous westerlies), with 22 eastward and 17 westward moving systems, while in all other phases (including the weak MJO category) the number of westward moving systems is slightly larger than the number of eastward systems.

After accounting for variations in TC numbers between different MJO phases, the spatial distribution and average latitude of formation is relatively similar for each of the different MJO phases. Similarly, the annual cycle of the MJO and the months in which each phase occurs is unable to explain this variability, noting that *Wheeler et al.* [2009] documented no obvious phase locking to calendar

Table 3. Summary of Figure 5[a]

	Phase 8 – 1		Phase 2 – 3		Phase 4 – 5		Phase 6 – 7		Weak		All	
% All Storms	10		14		25		17		35		100	
% E moving WEST/EAST	15	47	21	47	38	47	21	56	25	45	27	49
% E moving 0-12.5°S WEST/EAST	23	50	22	33	44	42	38	50	28	23	31	39
% E moving 12.5–25°S WEST/EAST	0	45	18	55	30	50	0	59	20	56	18	54

[a]Same as Table 2 but for storms in each MJO phase and for all phases.

date. Consequently, in contrast to the monthly analysis (Figure 4), the variations in TC track directions categorized based on MJO phases are unable to be explained by systematic variations in genesis location in relation to the coast or latitude of genesis. Rather than being associated with variations in TC formation, the influence of the MJO on TC track direction in the western region is likely associated with other factors such as variations of the broader-scale environmental conditions in response to the MJO.

Figure 6 presents the variation in the eastward component of the steering flow winds for different phases of the MJO, noting that the MJO can be characterized in part by its influence on the background wind conditions throughout the troposphere. The steering flow is calculated over latitudes from 20°S to 5°S as described in section 2.2. The largest eastward component to the steering flow occurs in phase 4 – 5 with 35% of the total flow being westerly in WEST. In contrast, during phase 8 – 1, the eastward component only accounts for about 20% of the steering flow. In EAST the largest eastward component occurs in phase 6 – 7, consistent with the percentage of eastward moving TCs in this phase.

The mechanism for the change in steering flow in different MJO phases can be explained by the vertical and longitudinal structure of the zonal wind anomalies associated with each of the MJO phases (Figure 7). These zonal wind anomaly composites are constructed by removing the seasonal cycle and averaging over all days that fall in a particular phase of the MJO. In phase 8 – 1, corresponding to suppressed convective activity in the Australia region (Table 1), the zonal wind anomalies are easterly in the WEST and westerly in the EAST, extending from the surface up to around the 500 hPa pressure level throughout the main portion of the

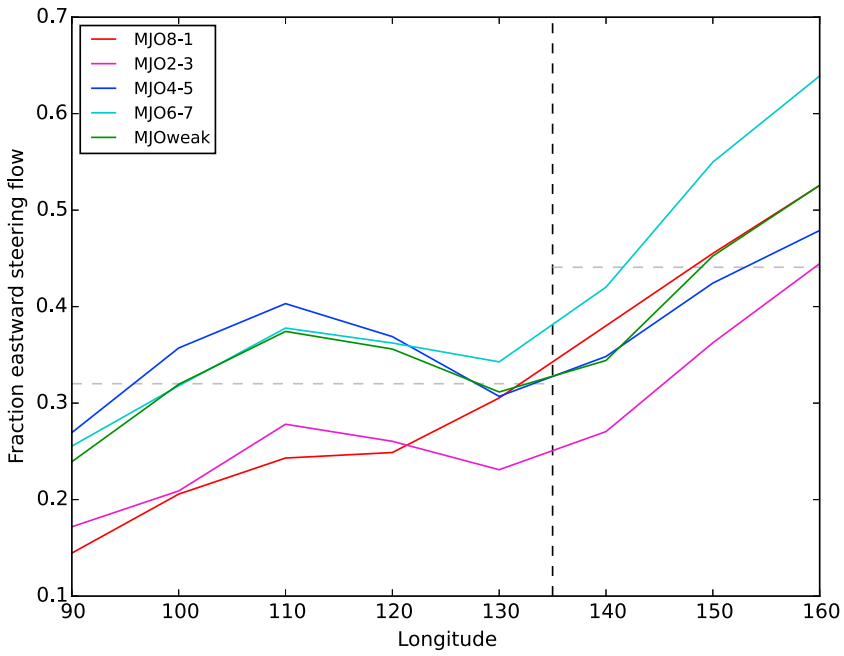

Figure 6. Fraction of the steering flow that is eastward in different phases of the MJO, during November–April, within the latitude range of 5°S and 20°S. The dashed horizontal lines show the mean for each region.

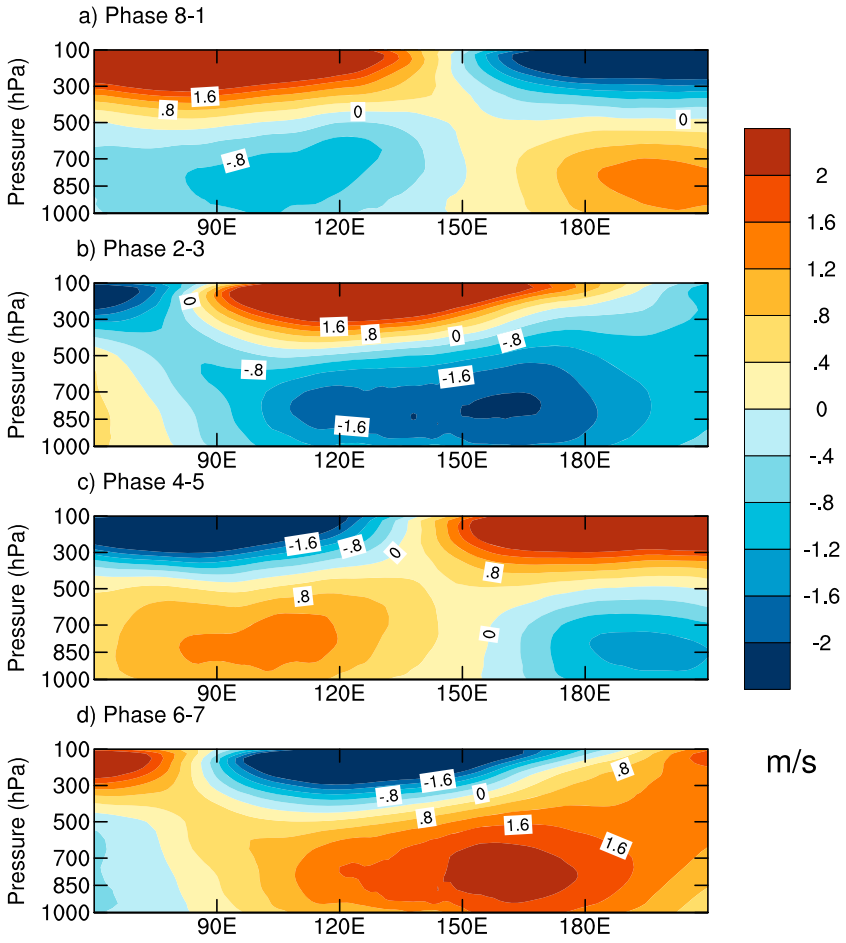

Figure 7. Composite longitude-pressure plots of zonal wind anomalies for different phases of the MJO, averaged over the latitude range of 5°S to 20°S during the study period.

atmosphere that drives TC motion [e.g., *Chan*, 2005]. The region of anomalous easterly flow propagates eastward as indicated by increasing phase numbers of the MJO. In phase 2 – 3, this anomalous westward flow extends over the Australian continent (from about 120°E to 150°E). In phase 4 – 5, anomalous westerly winds become apparent in the western part of the Australian region, resulting in a more prevalent eastward component of the steering flow (Figure 6) and an increased proportion of eastward moving TCs (Figure 5).

4. Discussion and Conclusions

Climatological examinations of TC activity in the Australian region were presented, with a particular focus on the variability of TC track directions. Climatological maps were shown detailing the full spectrum of TC track directions throughout the region (Figure 1), including the distribution of translational speed in each direction. The seasonal variability in TC track directions was also investigated, including an examination of the factors associated with this variability such as the influence of the MJO.

The benefits of considering the full spectrum of TC track directions rather than mean direction were clearly demonstrated, particularly in cases such as for the region near the Gulf of Carpentaria (around 140°E) where there was a nearly equal proportion of eastward to westward moving systems which cancel each other out in zonal direction when averaged together (Figure 1b). The track characteristics of the TCs presented here indicate that a longitude of 135°E represents a boundary between TCs that are more similar to those of western and eastern Australia, respectively. TC tracks west of this line tend to have a directional spectrum more dominated by a westward component than east of this line where there is an almost equal proportion of eastward and westward moving systems. Consequently, these results suggest the use of this line of 135°E longitude for

climatologically defining TC basin boundaries and characteristics, based on considerations of TC track directional variability.

It was demonstrated that there is a considerable degree of variability in TC track directions in this region. During the middle of the TC season (January–March), there is a greater proportion of westward moving TCs in the western basin, as well as eastward moving TCs in the eastern basin. This variation is consistent with a southward shift in the location of genesis during the middle of the TC season (Figure 4), consistent with the shift in the monsoon shear line, resulting in more systems with the potential to develop occurring closer to land, thereby favoring the formation of systems that remain over water due to motion away from the continent.

In addition to the aforementioned seasonal variations that are relatively fixed with respect to particular months within the TC season, the MJO was also found to influence TC track direction in the Australian region. This is a somewhat different result to that of *Hall et al*. [2001] who found no significant relationship between track direction and the phases of the MJO, while noting differences in the methodology used. *Hall et al*. [2001] used the average TC track direction over $10° \times 10°$ boxes, in contrast to the method used here which considers individual TC directions, as well as noting the longer time period of available data used. We demonstrated that the influence of the MJO on track directions in the western part of this region is consistent with MJO-related variations in the background environmental winds (steering flow). Anomalous eastward steering flow occurs during phase $4-5$ and anomalous westward flow during phase $8-1$ in WEST, with resulting changes in the proportion of TC tracks in each direction during these phases of the MJO.

In contrast to some previous studies that have used a cluster analysis method to classify TC tracks [*Chand and Walsh*, 2010; *Ramsay et al*., 2012], here we applied a relatively simple method of classification as either westward or eastward based on the initial net zonal motion during the first 48 h of the recorded track. While noting that there can be benefits to using a range of different analysis methods (e.g., depending on a specific purpose), the relative simplicity of the classification method used here reduces the risk of potentially introducing artifacts resulting from the use of highly complex methodologies and allows results to be easily reproduced.

The results presented here indicate a considerable degree of variation in TC tracks in this region, with plausible physical reasons for these variations being suggested. Consequently, this study indicates the potential for improved predictive capacity in relation to aspects of TC activity in this region, including in relation to TC track directions. It is intended that these results will be of use for providing guidance for operational predictive services in this region, as well as potentially forming the basis for the future development of predictive tools relating to TC track direction variability at intraseasonal time scales. Recent initiatives such as the Sendai Framework for Disaster Risk Reduction [*Aitsi-Selmi et al*., 2015] highlight that improved knowledge of the characteristics of extreme phenomena such as TC activity is important in a changing environment, particularly for improving predictive capacity to reduce risk and increase resilience to the impacts these events can have on various regions throughout the world.

There is a considerable scope for further investigations into the factors that influence TC track variations in this region, particularly on intraseasonal time scales. For example, the ability of dynamical and/or statistical predictive models to represent intraseasonal variations in TC track directions associated with the influence of the MJO on TC steering flow could be examined, with this representing a required step for assessing the applicability of the results presented here in an operational context. Additionally, the influence of the MJO on recurvature could also be investigated in relation to the observed intraseasonal variations in TC tracks in this region. Furthermore, as ENSO and the Indian Ocean Dipole (IOD) are dominant modes of variability on seasonal scales, with significant influences of background environmental conditions of relevance to the modulation of a number of different aspects of TC activity, the interactions between the MJO and these seasonal modes of variability could potentially be of importance in relation to an improved understanding of the drivers and predictability of variability in TC tracks.

Acknowledgments

This work was supported by the Australian Climate Change Science Programme, funded jointly by the Department of the Environment, the Bureau of Meteorology, and CSIRO. A.D. was supported through funding from the Australian Government's National Environmental Science Programme. The IBTrACs TC best track data were obtained from NOAA (http://www.ncdc.noaa.gov/ibtracs/index.php?name=-wmo-data) and the ERA-Interim data are available from ECMWF (http://apps.ecmwf.int/datasets/data/interim-full-daily/levtype=pl/). The RMM MJO data used in the paper are available from BoM (http://www.bom.gov.au/climate/mjo/graphics/rmm.74toRealtime.txt). We thank Matthew Wheeler, Benjamin Ng, Kevin Hennessy, Mike Fiorino, and two anonymous reviewers for their comments that helped to improve the manuscript.

References

Aitsi-Selmi, A., S. Egawa, H. Sasaki, C. Wannous, and V. Murray (2015), The Sendai framework for disaster risk reduction: Renewing the global commitment to people's resilience, health, and well-being, *Int. J. Disast Risk Sci.*, *6*(2), 164–176, doi:10.1007/s13753-015-0050-9.

Basher, R. E., and X. Zheng (1995), Tropical cyclones in the southwest Pacific: Spatial patterns and relationships to southern oscillation and sea surface temperature, *J. Clim.*, *8*, 1249–1260.

Bessafi, M., and M. C. Wheeler (2006), Modulation of south Indian Ocean tropical cyclones by the Madden–Julian Oscillation and convectively coupled equatorial waves, *Mon. Weather Rev.*, *134*, 638–656, doi:10.1175/MWR3087.1.
Bessafi, M., A. Lasserre-Bigorry, C. J. Neumann, F. Pignolet-Tardan, D. Payet, and M. Lee-Ching-Ken (2002), Statistical prediction of tropical cyclone motion: An analog-CLIPER approach, *Weather Forecast.*, *17*(4), 821–831.
Camargo, S. J., M. C. Wheeler, and A. H. Sobel (2009), Diagnosis of the MJO modulation of tropical cyclogenesis using an empirical index, *J. Atmos. Sci.*, *66*(10), 3061–3074, doi:10.1175/2009JAS3101.1.
Carr, L. E., and R. L. Elsberry (1990), Observational evidence for predictions of tropical cyclone propagation relative to environmental steering, *J. Atmos. Sci.*, *47*(4), 542–546.
Chan, J. C. L. (2005), The physics of tropical cyclone motion, *Annu. Rev. Fluid Mech.*, *37*(1), 99–128, doi:10.1146/annurev.fluid.37.061903.175702.
Chand, S. S., and K. J. E. Walsh (2010), The influence of the Madden-Julian oscillation on tropical cyclone activity in the Fiji region, *J. Clim.*, *23*(4), 868–886, doi:10.1175/2009JCLI3316.1.
Chand, S. S., and K. J. E. Walsh (2009), Tropical cyclone activity in the Fiji region: Spatial patterns and relationship to large-scale circulation, *J. Clim.*, *22*(14), 3877–3893, doi:10.1175/2009JCLI2880.1.
Chen, T. C., S. Y. Wang, M. C. Yen, and A. J. Clark (2009), Impact of the intraseasonal variability of the western North Pacific large-scale circulation on tropical cyclone tracks, *Weather Forecast.*, *24*(3), 646–666.
Dare, R. A., and N. E. Davidson (2004), Characteristics of tropical cyclones in the Australian region, *Mon. Weather Rev.*, *132*, 3049–3065.
Dee, D. P., et al. (2011), The ERA-Interim reanalysis: configuration and performance of the data assimilation system, *Q. J. R. Meteorol. Soc.*, *137*(656), 553–597.
Diamond, H. J., and J. A. Renwick (2014), The climatological relationship between tropical cyclones in the southwest pacific and the Madden-Julian Oscillation, *Int. J. Climatol.*, doi:10.1002/joc.4012.
Dowdy, A., and Y. Kuleshov (2012), An analysis of tropical cyclone occurrence in the Southern Hemisphere derived from a new satellite-era data set, *Int J Remote Sens*, *33*(23), 7382–7397.
Dowdy, A. J. (2014), Long-term changes in Australian tropical cyclone numbers, *Atmos. Sci. Lett.*, *15*(4), 292–298.
Dowdy, A. J., L. Qi, D. Jones, H. Ramsay, R. Fawcett, and Y. Kuleshov (2012), Tropical cyclone climatology of the south Pacific Ocean and its relationship to El Niño-Southern Oscillation, *J. Clim.*, *25*(18), 6108–6122, doi:10.1175/JCLI-D-11-00647.1.
Evans, J. L., and R. J. Allan (1992), El Niño/Southern Oscillation modification to the structure of the monsoon and tropical cyclone activity in the Australian region, *Int. J. Climatol.*, *12*(6), 611–623.
Frank, W. M., and P. E. Roundy (2006), The role of tropical waves in tropical cyclogenesis, *Mon. Weather Rev.*, *134*, 2397–2417.
Hall, J. D., A. J. Matthews, and D. J. Karoly (2001), The modulation of tropical cyclone activity in the Australian region by the Madden–Julian Oscillation, *Mon. Weather Rev.*, *129*(12), 2970–2982.
Harper, B. A., S. A. Stroud, M. McCormack, and S. West (2008), A review of historical tropical cyclone intensity in northwestern Australia and implications for climate change trend analysis, *Aust Meteorol Mag*, *57*, 121–141.
Ho, C. H., J. H. Kim, J. H. Jeong, H. S. Kim, and D. Chen (2006), Variation of tropical cyclone activity in the South Indian Ocean: El Niño–Southern Oscillation and Madden-Julian Oscillation effects, *J. Geophys. Res.*, *111*, D22101, doi:10.1029/2006JD007289.
Holland, G. L. (1984a), Tropical cyclone motion. A comparison of theory and observation, *J. Atmos. Sci.*, *41*(1), 68–75.
Holland, G. L. (1984b), On the climatology and structure of tropical cyclones in the Australian/southwest Pacific region: I. Data and tropical storms, *Aust. Met. Mag.*, *32*, 1–15.
Kim, J. H., C. H. Ho, H. S. Kim, C. H. Sui, and S. K. Park (2008), Systematic variation of summertime tropical cyclone activity in the western North Pacific in relation to the Madden-Julian oscillation, *J. Clim.*, *21*(6), 1171–1191.
Knapp, K. R., M. C. Kruk, D. H. Levinson, H. J. Diamond, and C. J. Neumann (2010), The International Best Track Archive for Climate Stewardship (IBTrACS), *Bull. Am. Meteorol. Soc.*, *91*(3), 363–376, doi:10.1175/2009BAMS2755.1.
Kuleshov, Y., L. Qi, R. Fawcett, and D. Jones (2008), On tropical cyclone activity in the Southern Hemisphere: Trends and the ENSO connection, *Geophys. Res. Lett.*, *35*, L14S08, doi:10.1029/2007GL032983.
Lavender, S. L., and D. J. Abbs (2013), Trends in Australian rainfall: Contribution of tropical cyclones and closed lows, *Climate Dynam.*, *40*(1-2), 317–326, doi:10.1007/s00382-012-1566-y.
Leroy, A., and M. C. Wheeler (2008), Statistical prediction of weekly tropical cyclone activity in the Southern Hemisphere, *Mon. Weather Rev.*, doi:10.1175/2008MWR2426.1.
Li, R. C., and W. Zhou (2013), Modulation of western North Pacific tropical cyclone activity by the ISO. Part II: Tracks and landfalls, *J. Clim.*, *26*(9), 2919–2930.
Liu, K. S., and J. C. L. Chan (2012), Interannual variation of Southern Hemisphere tropical cyclone activity and seasonal forecast of tropical cyclone number in the Australian region, *Int. J. Climatol.*, *32*(2), 190–202, doi:10.1002/joc.2259.
McBride, J., and T. Keenan (1982), Climatology of tropical cyclone genesis in the Australian region, *J Climatol*, *2*(1), 13–33.
Nicholls, N. (1979), A possible method for predicting seasonal tropical cyclone activity in the Australian region, *Mon. Weather Rev.*, *107*(9), 1221–1224.
Nicholls, N. (1984), The Southern Oscillation, sea surface temperature, and interannual fluctuations in Australian tropical cyclone activity, *J Climatol.*, *4*(6), 661–670.
Pike, C. A., and C. J. Neumann (1987), The variation of track forecast difficulty among tropical cyclone basins, *Weather Forecast.*, *2*, 237–241.
Productivity Commission (2014), Natural disaster funding arrangements Inquiry *Rep. 74*, Canberra.
Ramsay, H. A., L. M. Leslie, P. J. Lamb, M. B. Richman, and M. Leplastrier (2008), Interannual variability of tropical cyclones in the Australian region: Role of large-scale environment, *J. Clim.*, *21*(5), 1083–1103.
Ramsay, H. A., S. J. Camargo, and D. Kim (2012), Cluster analysis of tropical cyclone tracks in the Southern Hemisphere, *Climate Dynam.*, *39*(3), 897–917.
Robertson, A. W., A. Kumar, M. Peña, and F. Vitart (2015), Improving and promoting subseasonal to seasonal prediction, *Bull. Am. Meteorol. Soc.*, *96*(3), doi:10.1175/BAMS-D-14-00139.1.
Vitart, F. (2014), Evolution of ECMWF sub-seasonal forecast skill scores, *Q. J. R. Meteorol. Soc.*, *140*(683), 1889–1899.
Vitart, F., A. Leroy, and M. C. Wheeler (2010), A comparison of dynamical and statistical predictions of weekly tropical cyclone activity in the Southern Hemisphere, *Mon. Weather Rev.*, *138*, 3671–3682.
Werner, A., A. M. Maharaj, and N. J. Holbrook (2012), A new method for extracting the ENSO-independent Indian Ocean dipole: Application to Australian region tropical cyclone counts, *Clim. Dyn.*, *38*(11-12), 2503–2511.
Wheeler, M. C., and H. H. Hendon (2004), An all-season real-time multivariate MJO index: Development of an index for monitoring and prediction, *Mon. Weather Rev.*, *132*(8), 1917–1932.

Wheeler, M. C., H. H. Hendon, S. Cleland, H. Meinke, and A. Donald (2009), Impacts of the Madden-Julian Oscillation on Australian rainfall and circulation, , *J. Clim.*, *22*(6), 1482–1498.

Wu, L., Z. Ni, J. Duan, and H. Zong (2013), Sudden tropical cyclone track changes over the western North Pacific: A composite study, *Mon. Weather Rev.*, *141*(8), 2597–2610.

Yang, L., Y. Du, D. Wang, C. Wang, and X. Wang (2015), Impact of intraseasonal oscillation on the tropical cyclone track in the South China Sea, *Clim. Dyn.*, *44*(5-6), 1505–1519.

Zhang, C. (2013), Madden-Julian Oscillation: Bridging weather and climate, *Bull. Am. Meteorol. Soc.*, *94*, 1849–1870.

Zhao, H., L. Wu, and W. Zhou (2009), Observational relationship of climatologic beta drift with large-scale environmental flows, *Geophys. Res. Lett.*, *36*, L18809, doi:10.1029/2009GL040126.

Zhu, H., M. C. Wheeler, A. H. Sobel, and D. Hudson (2014), Seamless precipitation prediction skill in the tropics and extratropics from a global model, *Mon. Weather Rev.*, *142*, 1556–1569.